IRAQI JOURNAL OF APPLIED PHYSICS
Vol. 22, No. 1, January-March 2026, pp. 121-126

Wasan R. Saleh [1]
Kejeen M. Ibrahim [2]
Dhulfiqar S. Mutashar [3]

[1] Department of Physics, College of Science, University of Baghdad, Baghdad, IRAQ
[2] Department of Physics, College of Education for Pure Science Ibn AL-Haitham, University of Baghdad, Baghdad, IRAQ
[3] College of Applied Science, University of Technology, Baghdad, IRAQ
*Corresponding author: cajeen.m.i@ihcoedu.uobaghdad.edu.iq

ZnO Nanorods Synthesized by Hydrothermal Method and Doped with Nanomaterials (Au, Cu, Pt, Ni, and Gr): Structural Properties and Comparative Study

In this research, ZnO nanorods were successfully prepared using the hydrothermal method. Pure ZnO was doped with many nanoparticles 3% of (Au, Cu, Pt, Ni, and Gr), and the effect of these dopants on the structural and morphological properties. X-ray diffraction (XRD) showed the formation of hexagonal wurtzite structure crystal in all Pure and doped samples with an average particle size of ~11nm and some weak peaks of dopant crystalline nanoparticles (Au, Cu, Pt, Ni, and Gr). The surface morphology of undoped and doped ZnO with nanoparticles was investigated using scanning electron microscopy (SEM), and it was observed to be nanorod. Atomic force microscopy (AFM) images have shown that surface and morphology roughness were influenced by doping. FTIR spectroscopy has been used to investigate the functional groups in forming pure and doped ZnO.

Keywords: Zinc oxide; Nanorods; Nanoparticles; Structural properties
Received: 28 May 2025; Revised: 5 August; Accepted: 12 August; Published: 1 January 2026

1. Introduction

Zinc oxide (ZnO) is a semiconductor of an n-type, inorganic white powder with a great energy bandgap (3.37eV) and a large binding energy of the exciton (60 meV). ZnO has attracted interest in many applications and performs better than other semiconductors because of several benefits, including ease of manufacture, power electronics, optical properties, non-toxicity, and low cost. ZnO nanostructures are made using various techniques, including hydrothermal, sol-gel, laser ablation, etc. [1]. ZnO can possess three crystalline structures. Cubic zinc blende, cubic rock salt, ZnO, and hexagonal wurtzite structure are reported in the literature. The wurtzite structure is the most stable phase of ZnO. The hexagonal wurtzite ZnO unit cell comprises (Zn^{2+}) cation and is surrounded by four anions (O^{2-}) at the center of a tetrahedron [2,3]. Various techniques are used to make ZnO nanostructures including sol-gel, laser ablation, hydrothermal, and more. The hydrothermal method is gaining increasingly popular due to its safer, faster, more diverse, lower-cost, and offers better control [1].

To improve the photocatalytic activity of ZnO, several researchers have proceeded to minimize the energy gap of ZnO because of the large band gap of ZnO. The research involves the deposition of noble metal, doping metal and non-metal ions, and composite semiconductors. ZnO crystals doped with various transition metal ions led to improved properties of ZnO nanoparticles and performed better in applications [4]. Doping ZnO with elements such as Ni [5], Pt [6], Cu [7], and Au [8] allows for their effective development by enhancing efficiency and changing their activity to certain wavelength regions. Doping with transition metals or non-metals can deeply affect ZnO's optical, electrical, and magnetic behavior, making it convenient for considerable applications [5].

Novel studies have also shown nanocomposites based on graphene-decorated ZnO, which find an assortment of applications in fuel cells, sensors, light energy transformation, and catalysis. This is due to graphene's good stability, characteristics of excellent charge transfer, large specific surface area, outstanding electron transfer ability, low cost, and excellent electrocatalytic activity. Graphene and ZnO are good optical and electrical catalysts that could be further reinforced by the coupling of these two components [9].

In this work, a hydrothermal technique was used to prepare pure ZnO, which was then topped with Au, Cu, Pt, Ni, and Gr nanoparticles. This paper aims to study the impact of dopants on the morphologies and structures of pure ZnO by examining the effect of these

dopants on the structural properties and improvement for considerable applications.

2. Experimental Work

Table (1) displays the chemical materials used to prepare pure ZnO nanorods and ZnO doped with 3% of Au, Cu, Pt, Ni, and Gr nanoparticles.

A molecular weight (M.W.) of 219.5 g/mol of Zn $(CH_3COO)_2.2H_2O$ dissolved in 100 mL of methanol at room temperature and a molecular weight of 40 g/mol of NaOH dissolved in 500 mL of methanol were used to prepare ZnO nanorods. These two mixture solutions have been transported to stainless-steel autoclaves within a Teflon-lined. The reactor was tight and left for a temperature of 70 °C at a growth time of 6 hours. Then, the mixture was poured into a beaker and rinsed several times with distilled water and Ethanol alcohol at least three times. Finally, the nanorod powder was dried for 1 hour at 80 °C to have a product. At first, pure ZnO powder was ground in a mortar for about two minutes. After that, ZnO was dissolved in methanol and applied onto a cleaned glass substrate using the doctor's blade coating.

For the doped samples, nanoparticles of gold (Au), copper (Cu), platinum (Pt), nickel (Ni), and graphene (Gr) were used, each making up a 3% percentage. Based on previous experiments and laboratory research, this percentage was chosen.

Post-synthesis impregnation approach using an ultrasonic probe separated the nanoparticles, mixed them with 1 mL of methanol, and stirred for 5 minutes to create a uniform suspension. Similarly, ZnO was stirred with 1 mL of methanol to form a harmonious dispersion.

Finally, the suspensions of nanoparticles were individually added to the ZnO solution and stirred for 10 minutes to obtain a homogeneous mixture.

The samples were analyzed using several techniques to understand their structural properties. Their crystal structure was examined using X-ray diffraction (XRD) with a Lab XRD-6000 instrument. This involves using CuK-alpha radiation (wavelength of 1.54060Å) and settings of 30 mA current and 40 kV voltage. The samples were scanned at angles ranging from 5° to 80°. The surface morphology of the purr and doped ZnO nanorods was studied using the scanning electron microscopy (JSM-7610F Japan). Atomic force microscope (AFM) AA3000 analysis from Angstrom Advanced has been used to study the topography of the pure and doped ZnO nanorods. The functional groups and chemical bonds in the samples were identified using Fourier-transform infrared (FTIR) spectrometry and solid KBr discs, and the measurements were taken with a maximum resolution of 0.5 cm^{-1}.

3. Results and Discussion

The XRD patterns of the synthesized ZnO nanorods by hydrothermal method, Au, Cu, Pt, Ni and Gr doped ZnO are presented in Fig. (1). XRD study of ZnO nanorods characterize diffraction peaks at 31.97°, 34.64°, 36.52°, 47.9°, 56.85°, 63.05°, and 69.1° corresponding to planes (100), (002), (101), (102), (110), (103), and (112), respectively, confirming the hexagonal wurtzite structure of ZnO nanorods (JPCDS card no. 36-1451) [1]. Also, sharp peaks and no additional diffraction lines indicate that the synthesized ZnO nanorods have good crystallinity and do not contain impurities. The insertion of dopants in the crystal system leads to slight shifts of the characteristic diffraction peaks to the low 2θ angles and variation of the diffraction intensities. The structure also showed several weak peaks of dopant crystalline nanoparticles, marked with "*", at specific angles: around 2θ = 44.05° for the (200) plane of Au NPs, 44.15°, 44°and 44.05° for the (111) plane of Cu, Pt, and Ni NPs, respectively. Additionally, the characteristic peaks of graphene (Gr) appeared at 26.65° and 44°, corresponding to the (002) and (101) planes, respectively. The observed shifts in the diffraction peak positions can be attributed to variations in lattice parameters, where the XRD data enable detailed analysis of lattice cell parameters and crystallite size in the doped ZnO (table 2). The lattice constants a and c varied with doping, verifying the successful doping of ZnO. Undoped ZnO synthesized exhibited the smallest a and c lattice constants of 3.23004 and 5.15307 Å, while the addition of dopants in the ZnO structure observed a slight increase in the lattice constants. Au/ZnO and Cu/ZnO show the largest c-axis expansion, proportionate with their larger ionic radii. Due to the smaller radii of Ni and Pt, Ni/ZnO and Pt/ZnO exhibit weaker lattice changes. The minimal changes in Gr/ZnO (a=3.23140Å, c=5.19405Å) suggest Gr acts as a surface modifier and a lattice dopant. The size of ZnO nanorods was calculated by Debye-Scherrer formula [10]:

$$D = \frac{0.89\lambda}{\beta cos\theta} \quad (1)$$

where 0.89 is indicated to Scherer's factor, λ is the wavelength of the x-ray, θ is the Bragg's diffraction angle, and β is the full-width at half-maximum (FWHM) of a specific diffraction angle

The average crystallite size of the ZnO nanorods corresponding to the FWHM of the most intense and strong diffraction peaks at 31.97, 34.64, and 36.52° and that refer to (101), (002), and (101) planes was found to be 11.1 nm. The average crystallite size found for the Au, Cu, Pt, Ni, and Gr doped in the ZnO was 11.4, 12, 12, 11.2, and 11 nm, respectively.

The surface morphology of undoped and doped ZnO with Au, Cu, Pt, Ni, and Gr nanoparticles was investigated using SEM, and it was observed to be nanorod in nature. Figure (2a) displays the SEM images of an undoped ZnO sample with an average particle size of around 110.3 nm with a distribution arranged from 53.2 to 233.92 nm. The SEM images in Fig. (2b-f) show that the dopant nanoparticles are spherical with an

average particle size of 31.95, 36.87, 34.43, 48.32, and 32.55 nm, respectively, and appear to spread in the structure of the ZnO NRs. Au NPs (bright spots) may decorate nanorod surfaces and reduce length, while the diameter increases from Au-induced surface energy modification.

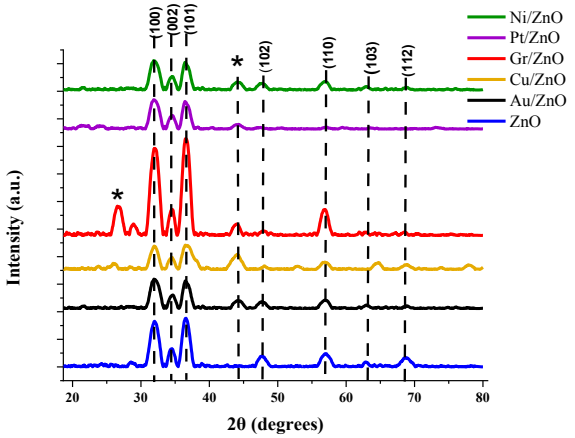

Fig. (1) XRD diffraction peaks of pure ZnO, doped ZnO with (Au, Cu, Pt, Ni, and Gr)

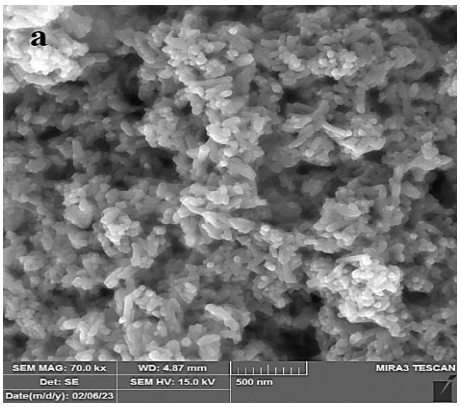

(a)

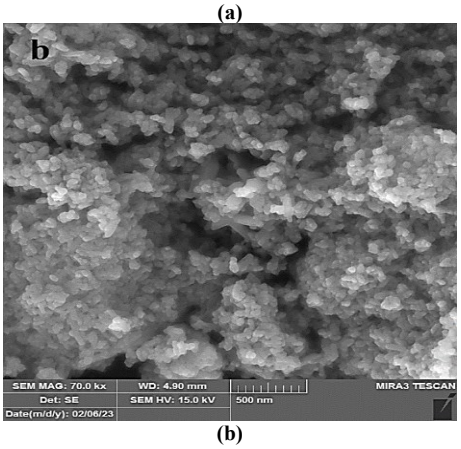

(b)

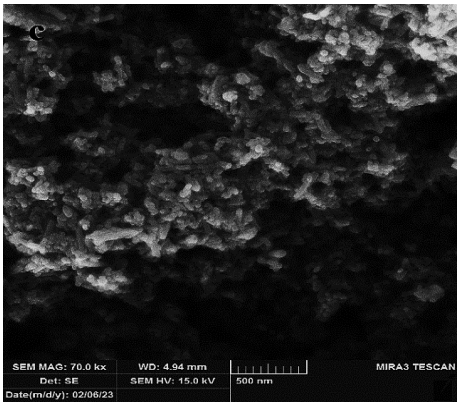

(c)

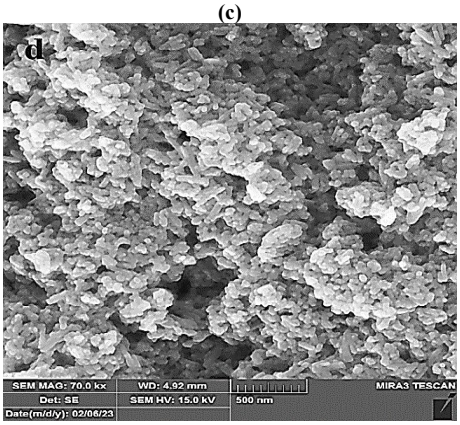

(d)

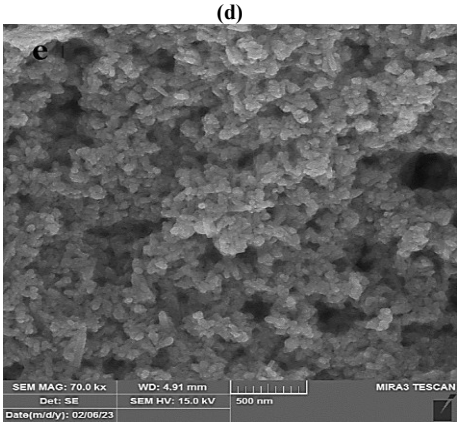

(e)

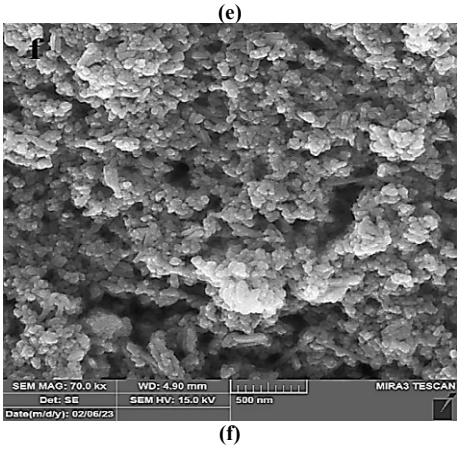

(f)

Fig. (2) SEM images of a (a) pure ZnO, (b) Au/ ZnO, (c) Cu/ZnO, (d) Pt /ZnO, (e) Ni /ZnO, and (f) Gr /ZnO films

Doping with copper (Cu) creates kinks or branched structures and random orientation with higher defect density (darker contrast in SEM). Pt nanoparticles (bright dots) appear isolated, minimizing rod distortion and slightly reducing nanorod length, while nanoparticles lead to tighter rod packing and rods losing sharpness. For Gr wrapped nanorods, bundling is caused, and crystallinity is reduced (broader XRD peaks). The SEM micrograph of doped ZnO shows a large aggregation of dopant nanoparticles, and particles appear in uniform and spherical shape. Undoped ZnO has a large particle size compared to ZnO doped with nanostructures (about 2 times). This observation is in good agreement with the AFM data analysis.

AFM is a powerful characterization tool for surfaces at the micro and nano level due to the instrument's superior resolution capabilities. The 3D AFM images scanned over a surface area of 1×1 μm^2 of pure ZnO and doped nanorods are further depicted in Fig. (3). It is seen that the morphology of ZnO nanorods is consistent with SEM observation. The detailed AFM parameters such as average roughness (Sa), root mean square roughness (Sq), ten-point height (Sz), and average particle size of the pure and doped ZnO are briefed in table (3). It is observed from the table, and the comparative study of Sa and Sq that the doped ZnO samples have less surface roughness, i.e., domains of small sizes are formed. Undoped ZnO exhibits the highest roughness Sq = 79.15nm, characteristic of pronounced growth of nanorods. Metallic dopants Au and Ni enhance smoothing and spectacular roughness reduction, Sq = 9.461nm and 12.03 nm for Au and Ni, respectively. This may be due to nanoparticles filling the inter-rod space.

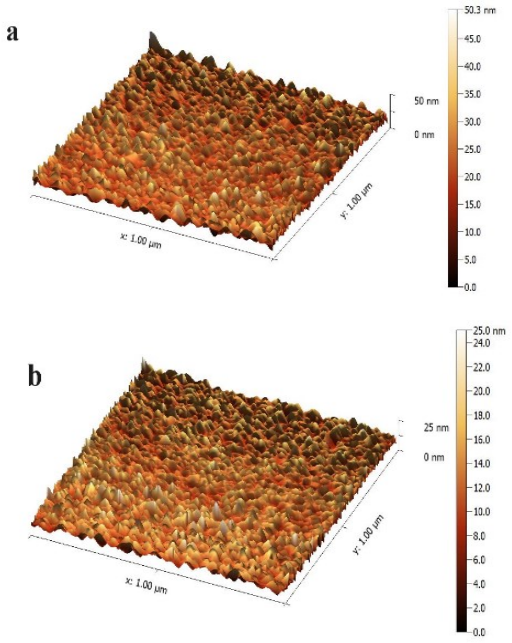

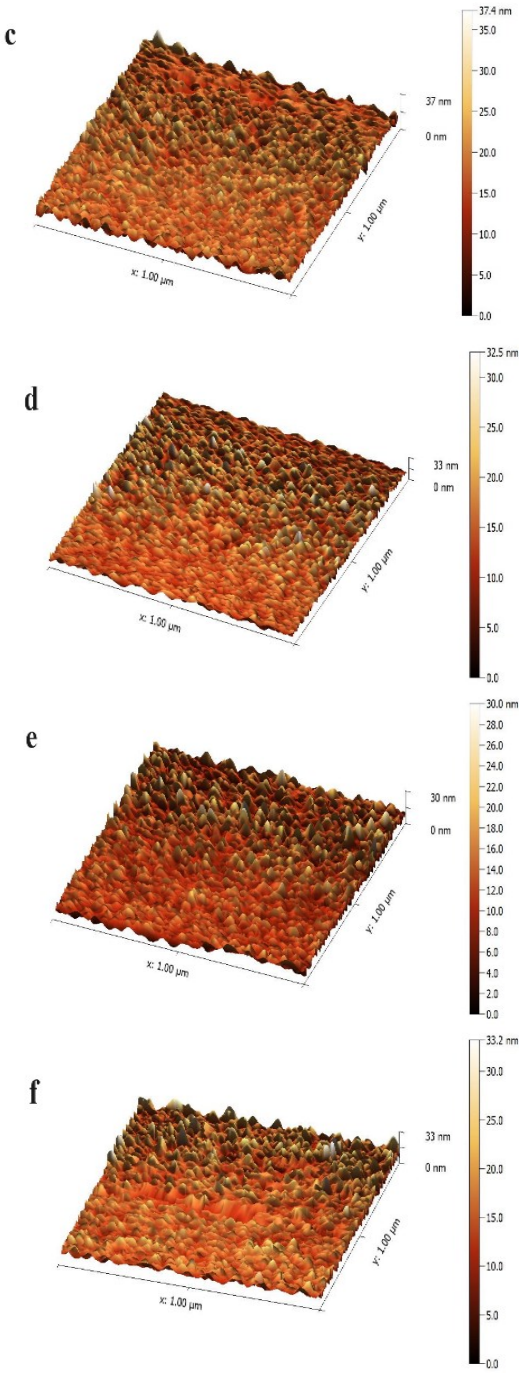

Fig. (3) The 3D AFM images for (a) pure ZnO NRs, (b) Au/ZnO, (c) Cu/ZnO, (d) Pt /ZnO, (e) Ni /ZnO, and (f) Gr /ZnO films

Gr dopant creates the smoothest surface, Sq = 7.561nm, through graphene wrapping and suppression of nanorod formation as shown in SEM observed particle distributions. While Cu/ZnO and Pt/ZnO have a higher roughness than other doped samples (Sq= 22.45 and 21.86 nm) because of the larger average particle size, and uneven nanoparticle distribution. At the same time, the height of the peaks of the material also decreases according to ten-point high values. The average particle size was measured to be 228.2, 42.86,

39.41, 53.94, 42.07, and 33.42 nm for pure and doped ZnO with Au, Cu, Pt, Ni, and Gr, respectively. The particle size decreased as ZnO was doped with dopant nanostructures [11].

Table (3) AFM parameters; average roughness (Sa), root mean square roughness (Sq), ten-point height (Sz), and average particle size (D_{ave}) of the undoped and doped ZnO with Au, Cu, Pt, Ni, and Gr nanostructures

Sample	Sa (nm)	Sq (nm)	Sz (nm)	D_{ave} (nm)
Pure ZnO	67.27	79.15	325	228.2
Au/ZnO	7.460	9.461	58.32	42.86
Cu/ZnO	12.91	22.45	208.5	39.41
Pt/ ZnO	15.34	21.86	144.3	53.94
Ni/ ZnO	9.297	12.03	75.99	42.07
Gr/ZnO	6.220	7.561	60.55	33.42

FTIR spectroscopy has been used to investigate the functional groups in forming pure and doped ZnO with Au, Cu, Pt, Ni, and Gr nanostructures. Figure (4) shows the FTIR spectra of all samples in the wavenumber range of 400-4000 cm^{-1}, which shows the existence of different functional groups and chemisorbed types in pure and doped ZnO. The peak appearing at 568 cm^{-1} indicates the existence of stretching Zn–O vibration. The peaks at 1037 to 1102 cm^{-1} correspond to the C–O vibration mode. Peaks at 1469 cm^{-1} and 1500 cm^{-1} for pure ZnO may indicate the presence of C=O groups [12].

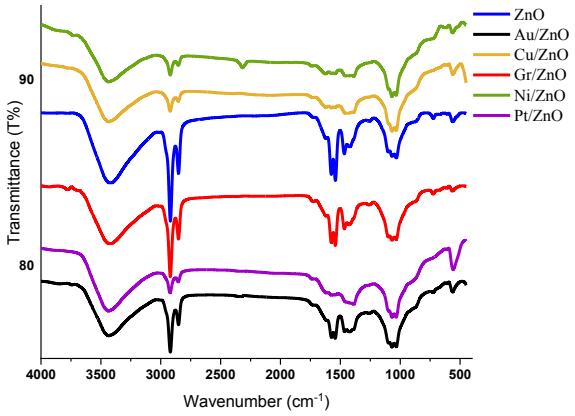

Fig. (4) FTIR spectra of pure ZnO, Au, Cu, Pt, Ni, and Gr doped ZnO nanorods

At various wavenumbers in the pure ZnO spectrum, the stretching vibration of the functional group C–H was also observed. Two peaks centered at 2909 cm^{-1} and 2920 cm^{-1} in the band correspond to symmetric and asymmetric modes, respectively [13].

The band around 3422 cm^{-1} agrees with the stretching vibration modes (O–H) of water molecules [14]. Compared to pure ZnO, the FTIR spectra of doped ZnO showed some changes, which may be because of the variance between the ionic radii of dopants and Zn^{2+}, which leads to the existence of a shift in the transmittance of the spectra and assists the substitution of Zn^{2+} by ions of dopants. There are no major new peaks for the Au/ZnO sample, but they can influence surface charge density and adsorbed species. There is a slight shift in the Zn-O stretching band for Cu/ZnO and Ni/ZnO samples, indicating substitutional doping. Also, peaks are enhanced at 1000-1300 cm^{-1}. In Pt/ZnO, the Zn-O band sharpens and blueshifts, indicating Pt substitution, and the peak at 1650 cm^{-1} disappears. Gr dopant affected ZnO structure, where the new peak appeared at 1585 cm^{-1} (C=C), graphene with sp^2. This also confirms the combination of dopants in the ZnO lattice.

4. Conclusions

In this article, ZnO nanorods were successfully synthesized using a hydrothermal technique and subsequently doped with Au, Cu, Pt, Ni, and Gr nanoparticles. The hexagonal wurtzite structure of ZnO nanorods was confirmed. The average crystallite size was found to be 11.1-12 for the pure and doped ZnO nanorods. Metallic dopants produced surface modifications and varying aggregations. The existence of various functional groups and chemisorbed species in undoped and doped ZnO nanorods was revealed. The doped ZnO showed the existence of a shift in the transmittance of the spectra which confirms the combination of dopants in the ZnO lattice. Doping ZnO nanorods with nanoparticles modified the structural and morphological properties, which developed their efficiency in many optoelectronic and photocatalytic applications.

References

[1] K.M. Ibrahim and W.R. Saleh, "ZnO nanostructures as low concentration NO_2 gas sensor and impact the temperature on sensing properties", in *AIP Conf. Proc.*, 2922(1) (2024).

[2] S. Vlassov et al., "Critical review on experimental and theoretical studies of elastic properties of wurtzite-structured ZnO nanowires", *Nanotech. Rev.*, 12(1) (2023) 20220505.

[3] K.M. Ibrahim, W.R. Saleh, and A.M. A. Al-Sammarraie, "Structural and Optical Properties of ZnO Nanostructures Synthesized by Hydrothermal Method at Different Conditions", *Nano Hybrid Comp.*, (35) (2022) 75–83.

[4] A.F. El-Sayed et al., "Synthesis, structural, molecular docking, and in vitro biological activities of Cu-doped ZnO nanomaterials", *Sci. Rep.*, 14(1) (2024) 9027.

[5] S.H. Zyoud et al., "Facile synthesis of Ni-doped ZnO nanostructures via laser-assisted chemical bath synthesis with high and durable photocatalytic activity", *Crystals (Basel)*, 13(7) (2023) 1087.

[6] A. Mezni et al., "Pt–ZnO/M (M= Fe, Co, Ni or Cu): A New Promising Hybrid-Doped Noble

Metal/Semiconductor Photocatalysts", *J. Inorg. Org. Polym. Mater.*, (30) (2020) 4627–4636.
[7] R. Sonkar et al., "Cu doped ZnO nanoparticles: Correlations between tuneable optoelectronic, antioxidant and photocatalytic activities", *J. Phys. Chem. Sol.*, 185 (2024) 111715.
[8] M. Alheshibri et al., "Tuning the morphology of Au/ZnO nanocomposite using pulsed laser ablation for anticancer applications", *Arab. J. Sci. Eng.*, 49(1) (2024) 1063–1074.
[9] L.Z. Yahiya and M.K. Dhahir, "Enhanced Physical Absorption Properties of ZnO Nanorods by Electrostatic Self-Assembly with Reduced Graphene Oxide and Decorated with Silver and Copper Nanoparticles", *Iraqi J. Phys.,* 19(48) (2025) 66-78.
[10] T. Seydioglu et al., "Effect of foreign impurity and growth temperatures on hexagonal structure and fundamental properties of ZnO nanorods", *Microscop. Res. Tech.*, 87(11) (2024) 2687-2700.
[11] A.Y. Taradh and W.R. Saleh, "Fabrication and characterization of functionalized multi-wall carbon nanotubes flexible network modified by a layer of polypyrrole conductive polymer and metallic nanoparticles", *Nano Hybrid Comp.*, 36 (2022) 21–33.
[12] I. Ngom et al., "On the use of Moringa oleifera leaves extract for the biosynthesis of NiO and ZnO nanoparticles", *MRS Adv.*, 5(21-22) (2020) 1145–1155.
[13] S.B. Rana and R.P.P. Singh, "Investigation of structural, optical, magnetic properties and antibacterial activity of Ni-doped zinc oxide nanoparticles", *J. Mater. Sci.: Mater. Electron.*, 27 (2016) 9346–9355.
[14] I. Ben Elkamel et al., "High responsivity and 1/f noise of an ultraviolet photodetector based on Ni doped ZnO nanoparticles", *RSC Adv.*, 8(56) (2018) 32333–32343.

Table (1) Materials used for the preparation of pure ZnO nanorods and ZnO doped with Au, Cu, Pt, Ni, and Gr NPs

Chemical Materials	Specifications	origin
Zinc acetate dehydrate ($Zn(CH_3COO)_2.2H_2O$	Purity 98 %, molecular weight of 219.49 g/mol	E. Merck Darmstadt Co. Germany
NaOH	Purity 99%, molecular weight of 40 g/mol	Applichem GmbH
Au NPs	purity of >99.97%, APS of 28nm, bulk density ~ 0.85 g/m^3	US Research Nanomaterials, Inc.
Cu NPs	purity of 99.9%, APS of 30 nm, Specific surface area 15 (m^2/g)	Nanjing High Technology Nano Material Co., Ltd.
Pt	purity of 99.9%, nanopowder < 25 nm	Nanografi Co.
Ni NPs	purity of 99.9%, nanopowder < 100nm, metals basis	Aldrich.
Gr	purity of >99.5+ %, 28 nm	US Research Nanomaterials, Inc.

Table (2) Parameters obtained from XRD patterns of ZnO NRs doped ZnO with (Au, Cu, Pt, Ni, and Gr)

Sample	2θ (Deg.)	FWHM (Deg.)	d_{hkl} Exp.(Å)	C.S (nm)	hkl	*a* (Å)	*c* (Å)	D (nm)
ZnO	31.97	1	2.7973	8.3	(100)	3.23004	5.15307	11.1
	34.64	0.57	2.5874	14.6	(002)			
	36.52	0.8	2.4584	10.5	(101)			
Au/ZnO	31.92	1	2.8014	8.3	(100)	3.23481	5.21197	11.4
	34.52	0.61	2.5962	13.6	(002)			
	36.38	0.68	2.4676	12.3	(101)			
Cu/ZnO	31.84	0.8	2.8083	10.3	(100)	3.24273	5.21685	12
	34.52	0.61	2.5962	13.7	(002)			
	36.45	0.7	2.46329	11.9	(101)			
Gr/ZnO	31.95	0.74	2.79848	11.2	(100)	3.23140	5.19405	12
	34.59	0.61	2.5911	13.6	(002)			
	36.44	0.75	2.4636	11.2	(101)			
Pt/ZnO	31.9	0.9	2.8031	9.2	(100)	3.23679	5.20100	11.2
	34.64	0.67	2.5874	12.4	(002)			
	36.38	0.7	2.4676	11.9	(101)			
Ni/ZnO	31.94	0.9	2.7997	9.2	(100)	3.23284	5.18002	11
	34.58	0.65	2.5918	12.8	(002)			
	36.45	0.75	2.4630	11.2	(101)			

